JOURNAL OF Materials CHEMISTRY

Crystal structures and luminescence properties of $La_3Zr_4F_{25}$ and α-$LaZr_3F_{15}$

Jeannette Dexpert-Ghys,[a] Sidney J. L. Ribeiro,[b] Pierre Dugat[c] and Daniel Avignant[c]

[a]*CEMES CNRS, BP 4347, 31055 Toulouse Cedex 4, France*
[b]*Instituto de Quimica, UNESP, P.O. BOX 355, 14800–900 Araraquara, S.P. Brasil*
[c]*Laboratoire des Matériaux Inorganiques, UPRES A-6002 CNRS, Université Blaise Pascal, 63177 Aubiere Cedex, France*

During a study of the LaF_3–ZrF_4 system, both $La_3Zr_4F_{25}$ and α-$LaZr_3F_{15}$ compounds have been evidenced. Their crystal structures have been determined from single-crystal X-ray diffraction data. $La_3Zr_4F_{25}$ crystallises in the cubic system with $a=$ 12.384 Å and $I\bar{4}3d$ space group (no. 220). Its crystal structure is built up of $(ZrF_6)^{2-}$ octahedra and $(LaF_8)^{5-}$ dodecahedra sharing corners. The low temperature form, α, of $LaZr_3F_{15}$ is orthorhombic (space group *Pmmn*, no. 59) with $a=15.721$ Å, $b=16.299$ Å, $c=8.438$ Å. Its structure is built of corner-sharing tricaped trigonal prisms surrounding the La^{3+} ions and both octahedra and monocapped trigonal prisms encompassing the Zr^{4+} ions. This structure is characterised by dynamically disordered $(ZrF_6)^{2-}$ complex anions.

The Eu^{3+} luminescence properties of these phases have been investigated and are discussed in relationship with their crystal structures.

Introduction

In a recent work dealing with the structure and the crystallisation of lanthanum fluorozirconate glasses[1] we mentioned the existence of a low temperature form, α, of $LaZr_3F_{15}$ of orthorhombic symmetry, as well as the presence of a phase, called 'X', of unknown structure appearing in annealed samples obtained from glassy compositions. This last phase 'X' has now been identified as $La_3Zr_4F_{25}$, from the crystal structure determination carried out on a single-crystal extracted from a glassy composition partially recrystallised. Furthermore, the crystal structure of the orthorhombic low temperature form α-$LaZr_3F_{15}$ has been determined. The present paper deals with the crystal structures of both $La_3Zr_4F_{25}$ and α-$LaZr_3F_{15}$ and the luminescence properties of these phases, in which Eu^{3+} was partially substituted for La^{3+}, analysed in relationship with their structures.

Experimental

Synthesis and preliminary crystallographic studies

$La_3Zr_4F_{25}$. A small fragment taken from a crushed annealed sample of a glassy composition $(1-x)ZrF_4$–$x(La_{0.95}Eu_{0.05})F_3$ with $x=0.4$ was selected and investigated using a Nonius CAD4 automatic diffractometer. The cubic unit cell with $a=$ 12.384(2) Å was obtained from the least-squares refinement of the measured setting angles of 25 reflections centred on the diffractometer for $5<\theta<19°$. Preliminary crystallographic study showed that the only space group compatible with the body centred lattice and the extinction conditions (*hhl*: $l=2n$ and $2h+l=4n$; 0*kl*: $k+l=2n$) should be $I\bar{4}3d$ (no. 220). The intensities were recorded in the conditions mentioned in Table 1.

α-$LaZr_3F_{15}$. Single crystals suitable for a structural study were obtained from a stoichiometric mixture of the starting LaF_3 and ZrF_4 fluorides heated at 750 °C in a sealed platinum tube and then cooled to room temperature at a rate of 6 °C h^{-1}. A very regular, almost spherical single crystal was selected and a preliminary study was carried out using precession photographs. It showed the symmetry to be orthorhombic with unit cell dimensions $a=15.721$ Å, $b=16.299$ Å and $c=8.438$ Å. The systematic extinctions lead to possible *Pmmn* or $Pmn2_1$ space groups. The intensities were recorded under the conditions mentioned in Table 1. Lorentz and polarisation corrections were applied followed by an absorption correction. All the programs used for data reduction and the structure determination were issued from the CAD4 SDP package.[2]

Spectroscopy

Eu^{3+} emission time resolved and excitation spectra were recorded at 77 K under excitation by a Nd-YAG (Spectra-Physics Quanta Ray DCR-4) pumped dye laser (Jobin Yvon E1T). For some experiments a Fabry–Perrot filter was introduced in the laser beam path to achieve a better selectivity of excitation in the $^7F_0 \rightarrow {}^5D_0$ range. The detection set-up, based on a digital oscilloscope interfaced with a microcomputer, allows to record several time-resolved spectra during one single scan, each of them characterised by the observation time delay after the pulse and the observation time gate. Fluorescence transients were recorded with the same set-up.

Crystal structure and luminescence of $La_3Zr_4F_{25}$

Structure determination

The structure was solved from the Patterson function and the fluorine positions were deduced from a difference Fourier synthesis which revealed firstly two independent fluorine ions in general 48e Wyckoff positions. Provided that the electroneutrality was almost achieved with these 96 F^- ions and that there are no sites of low multiplicity (ideally 4) available in the $I\bar{4}3d$ space group to complete the anionic sublattice, the presence of a small amount of oxygen in the sample could have been envisaged to balance the cationic charges (100+). This was not unreasonable taking into account the sample preparation, although this was carried out in a glove box under a dry argon atmosphere, because of the sensitivity of the zirconium tetrafluoride, and fluorides in general, to oxidation. However, careful examination of a new difference Fourier synthesis calculated subsequently to the anisotropic refinement of the two initial fluorine positions revealed residual

Table 1 Crystallographic data and data collection parameters for $La_3Zr_4F_{25}$ and α-$LaZr_3F_{15}$

	$La_3Zr_4F_{25}$	α-$LaZr_3F_{15}$
F_w	1256.6	697.55
symmetry	cubic ($I\bar{4}3d$)	orthorhombic ($Pmmn$)
lattice parameter(s)/Å	$a=12.384(2)$	$a=15.721(1)$ $b=16.299(2)$ $c=8.438(3)$
volume/Å^3	1899.4(6)	2162.2(6)
formulae per unit cell	4	8
calculated density/g cm^{-3}	4.394	4.285
crystal size mm	$0.12\times0.25\times0.07$	$0.17\times0.19\times0.15$
radiation, λ/Å	Mo-Kα (0.71069)	Mo-Kα (0.71069)
linear absorption coefficient, μ/mm^{-1}	8.93	6.86
absorption correction: empirical *via* ψ-scans on reflections series	(7 $\bar{2}$ 1)($\bar{4}$ 0 2) (7 $\bar{1}$ 2)	(0 4 0) (1 7 0) (0 12 2)
scan mode	ω–2θ	ω–2θ
width/°	$0.80+0.35\tan\theta$	$0.80+0.35\tan\theta$
aperture/mm	$2.70+0.40\tan\theta$	$2.70+0.40\tan\theta$
range measured	$1°<\theta<45°$ $-21<h<21$ $-21<k<21$ $0<l<21$	$1°<\theta<45°$ $0<h<22$ $0<k<22$ $0<l<21$
period of intensity control	3600 s, $\sigma=0.02$	3600 s, $\sigma=0.02$
observed reflections	4546	3553
independent reflections with $I>3\sigma(I)$	178	2610
R_{int} (from averaging)	0.034	
number of variables	30	218
secondary extinction parameter	$-2.13(5)\times10^{-8}$	$8.7(1)\times10^{-8}$
goodness of fit	0.706	1.373
residual electron density in final Fourier-difference synthesis/Å^{-3}	+0.483, −0.296	+2.824, −2.560
R; R_w	0.023; 0.025	0.037; 0.040

Table 2 Positional parameters for $La_3Zr_4F_{25}$

atom	Wyckoff position	occupancy	x	y	z	B_{iso}/Å
La	12a	1.000	3/8	0	1/4	1.98(1)
Zr	16c	1.000	0.33030(8)	x	x	2.52(1)
F(1)	48e	1.000	0.1674(6)	0.3178(6)	0.3185(6)	3.7(1)
F(2)	48e	0.950	0.2920(7)	0.4696(7)	0.3920(9)	6.8(3)
F(3)	24d	0.113	0.041(3)	0	1/4	5(1)

electron density. Therefore, a third anionic site F(3), corresponding to the 24d Wyckoff position with a low occupancy rate, was introduced. This improved substantially the discrepancy R factor which decreased from 0.043 to 0.023. As the F(2)–F(3) resulting contact distances were too short, the occupancy of the F(2) site was also decreased in such a way that both F(2) and F(3) occupancies allowed electroneutrality to be achieved, the F(1) site being fully occupied. The best result obtained is reported in Table 2. The main interatomic distances and angles are gathered in Table 3.

Europium spectroscopy

Only one type of europium fluorescence spectrum was observed in the $La_3Zr_4F_{25}$ phase. As was pointed out in a previous work,[1] it was recorded on the transparent part of a 0.6 ZrF_4–0.4 $(La_{0.95}Eu_{0.05})F_3$ sample quenched from the melt and assigned to the so-called F_x phase, now known as $La_3Zr_4F_{25}$. The $^5D_0\rightarrow{}^7F_1$ emission is characterised by a weak splitting between the three observed components and four lines were identified in the $^5D_0\rightarrow{}^7F_2$ region (Fig. 1). The Eu^{3+} $^5D_0$ lifetime is 6.3 ms.

Discussion

If the existence of a third anionic site called F(3), as mentioned previously, is likely, the nature of the species occupying this site is questionable as the corresponding Zr–F(3) distance is long [Zr–F(3) = 2.376 Å] for a fluorine ion but not exceptional for a bridging fluorine,[3,4] nor for an oxygen, particularly if this oxygen is involved in hydrogen bonding or belongs to a hydroxyl group.

So the eventuality that this third anionic position, which is necessary to balance the cationic charges assuming that no oxygen atoms are present on either F(1) or F(2) sites, would be occupied by oxygen or hydroxyl ions or by fluorine ions, has been envisaged. An argument in favour of fluorine ions in this anionic position is supplied by the existence of BaU_5LnF_{25} (Ln = La→Lu, Y) phases.[5] Writing the formula $Ba^{II}U^{IV}Ln^{III}U^{IV}{}_4F_{25}$, it clearly appears that the couple Ba^{2+}–U^{4+} may be substituted by two Ln^{3+} ions leading to the formula $Ln_3U_4F_{25}$, homologous with $La_3Zr_4F_{25}$. This may indicate that a pure fluorinated composition may be achieved for this stoichiometry. However the BaU_5LnF_{25} phases are isotypic with CsU_6F_{25}[6] and do not exhibit the same structure as $La_3Zr_4F_{25}$. So, whatever the true nature of the anion occupying this 24e third anionic site (if it is not an artefact) its role in the structure is not clear. Indeed, if we take this anionic position into account, it plays the role of a shared corner between two zirconium polyhedra, whereas without this anionic position [F(3) and F(2) positions are mutually exclusive], the zirconium polyhedra are isolated from one another (see Fig. 2) and linked only to the lanthanum polyhedra by corner sharing. Thus, surrounded by six anions, the zirconium is in a slightly distorted octahedral coordination (Fig. 3).

The La^{3+} ions occupy the 12a position and are in a dodecahedral coordination with a mean La–F distance of 2.372 Å, shorter than Shannon's distance[7] which is equal to 2.51 Å for eight-coordination of this ion. The observation of a unique environment for Eu^{3+} is in agreement with the structure resolved for $La_3Zr_4F_{25}$. The point symmetry at the 12a site is S_4. Whereas 0, 2 and 4 lines might be expected for the $^5D_0\rightarrow{}^7F_0$, $^7F_1$, $^7F_2$ emissions respectively, 0, 3 and 4 lines have been observed. It appears that the S_4 symmetry is slightly modified at the Ln^{3+} site by the anionic repartition. Since only F(1) and F(2) anionic positions are to be considered in the lanthanide coordination polyhedron, the eventual partial occupancy of the F(2) site by oxygen ions, which could be at the origin

Table 3 Main interatomic distances (Å) and angles (°) in $La_3Zr_4F_{25}$

La polyhedron [8] (mean La–F = 2.372 Å)

La	F(1)	F(1)	F(1)	F(1)	F(2)	F(2)	F(2)	F(2)
F(1)	**2.344(7)**	4.47(1)	3.46(1)	3.46(1)	4.51(1)	2.74(1)	2.94(1)	2.91(1)
F(1)	145.3(3)	**2.344(7)**	3.46(1)	3.46(1)	2.74(1)	4.51(1)	2.91(1)	2.94(1)
F(1)	95.1(3)	95.1(3)	**2.344(7)**	4.47(1)	2.94(1)	2.91(1)	2.74(1)	4.51(1)
F(1)	95.1(3)	95.1(3)	145.3(3)	**2.344(7)**	2.91(1)	2.94(1)	4.51(1)	2.74(1)
F(2)	144.1(3)	70.7(3)	76.6(3)	75.7(3)	**2.401(9)**	2.87(1)	4.35(1)	4.35(1)
F(2)	70.7(3)	144.1(3)	75.7(3)	76.6(3)	73.4(4)	**2.401(9)**	4.35(1)	4.35(1)
F(2)	76.6(3)	75.7(3)	70.7(3)	144.1(3)	130.0(3)	130.0(3)	**2.401(9)**	2.87(1)
F(2)	75.7(3)	76.6(3)	144.1(3)	70.7(3)	130.0(3)	130.0(3)	73.4(4)	**2.401(9)**

Zr polyhedron [6] (mean Zr–F = 1.986 Å)

Zr	F(2)	F(2)	F(2)	F(1)	F(1)	F(1)	F(3)	F(3)	F(3)
F(2)	**1.945(9)**	2.70(1)	2.70(1)	3.37(1)	2.60(1)	3.87(1)	2.64(1)	3.95(3)	1.80(4)
F(2)	87.9(4)	**1.945(9)**	2.70(1)	3.87(1)	3.37(1)	2.60(1)	1.80(4)	2.64(1)	3.95(3)
F(2)	87.9(4)	87.9(4)	**1.945(9)**	2.60(1)	3.87(1)	3.37(1)	3.95(3)	1.80(4)	2.64(1)
F(1)	115.8(4)	81.6(3)	153.4(4)	**2.028(7)**	2.64(1)	2.64(1)	4.22(1)	2.86(1)	2.49(2)
F(1)	153.4(4)	115.8(4)	81.6(3)	81.2(3)	**2.028(7)**	2.64(1)	2.49(2)	4.22(1)	2.86(1)
F(1)	81.6(3)	153.4(4)	115.8(4)	81.2(3)	81.2(3)	**2.028(7)**	2.86(1)	2.49(2)	4.22(1)
F(3)	74.5(9)	131.9(4)	47.9(4)	146.4(5)	68.4(2)	80.4(9)	**2.376(8)**	4.07(3)	4.07(3)
F(3)	47.9(4)	74.5(9)	131.9(4)	68.4(2)	80.4(9)	146.4(5)	117.8(9)	**2.376(8)**	4.07(3)
F(3)	131.9(4)	47.9(4)	74.5(9)	80.4(9)	146.4(5)	68.4(2)	117.8(9)	117.8(9)	**2.376(8)**

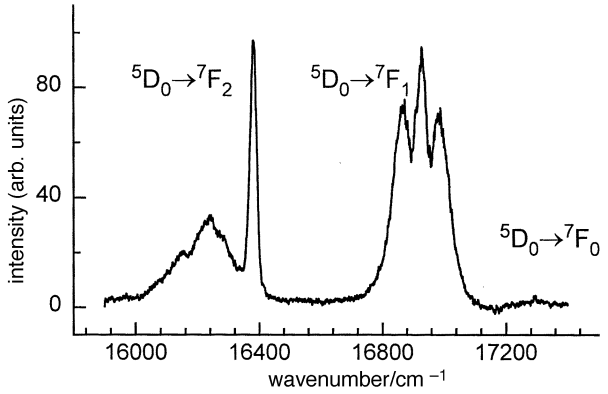

Fig. 1 $^5D_0 \rightarrow {}^7F_{1,2}$ emission spectrum recorded at 77 K, on $La_3Zr_4F_{25}:Eu^{3+}$, under excitation at 19043 cm^{-1}. The spectrum is the difference (data at long delay after pulse − data at short delay) calculated in order to remove the $^5D_1 \rightarrow {}^7F_{3,4}$ emissions.

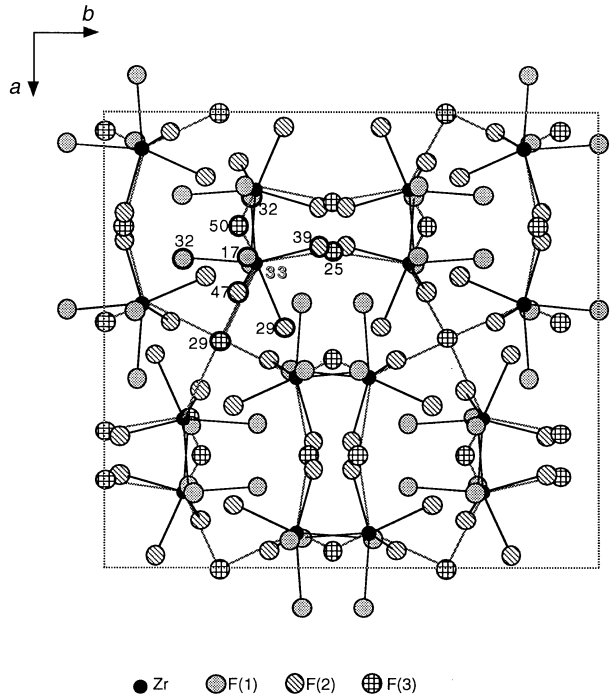

Fig. 2 Partial view of the structure of $La_3Zr_4F_{25}$ showing the Zr^{4+} polyhedra arrangement

of the symmetry breaking, has to be reconsidered here. However, it must be noticed that the observed lifetime is in agreement with those reported for Eu^{3+} in fluorinated matrices,[1] confirming that the percentage of oxygen ions in this position is really very low if any. An alternative explanation, taking into account the third anionic site, is as follows. As mentioned previously, the mutually exclusive occupation of two adjacent F(2) and F(3) positions leads also to a breaking of the S_4 symmetry at the La^{3+} site by introduction of a vacancy at the F(2) position if the adjacent F(3) one is occupied, whatever the nature of the species lying on the F(3) site.

The La polyhedra are isolated relative to each other with an La–La separation of 5.79 Å (Fig. 4). If, for simplification, the F(3) site is disregarded, the three-dimensional structure is built of Zr octahedra and La dodecahedra sharing corners in such a way that each La dodecahedron is linked to eight Zr octahedra (Fig. 5) and each Zr octahedron is linked to six dodecahedra.

Crystal structure and luminescence of α-$LaZr_3F_{15}$

Structure determination

The heavy La and Zr atoms were located from the three-dimensional Patterson function. The refinement of the cationic positions in the centric conventional *Pmmn* (no. 59) space group leads to satisfactory homogeneous thermal parameters for all the cations except for Zr(2) which exhibited a temperature factor about four times higher than the others. The splitting of the 2a site of the Zr(2) in a half-occupied 4f site improved the temperature factor which became of the same order of magnitude as those of the other cations and resulted in a decrease of the reliability factors. Attempts to refine these cationic positions in the acentric space group did not bring out any improvement. Therefore the structure refinement was carried out in the centric space group with the Zr(2) atom in a half-occupied site. Subsequent Fourier-difference syntheses allowed a large number of anions to be located unambiguously. However, the Fourier-difference maps also exhibited electron density anomalies located in the neighbourhood of cationic sites, in particular the Zr(2) ones.

Similar observations have been made by Laval *et al.* in the crystal structure determination of the $Ba_{4-z}Zr_{2+z/2}F_{16}$ phase[8]

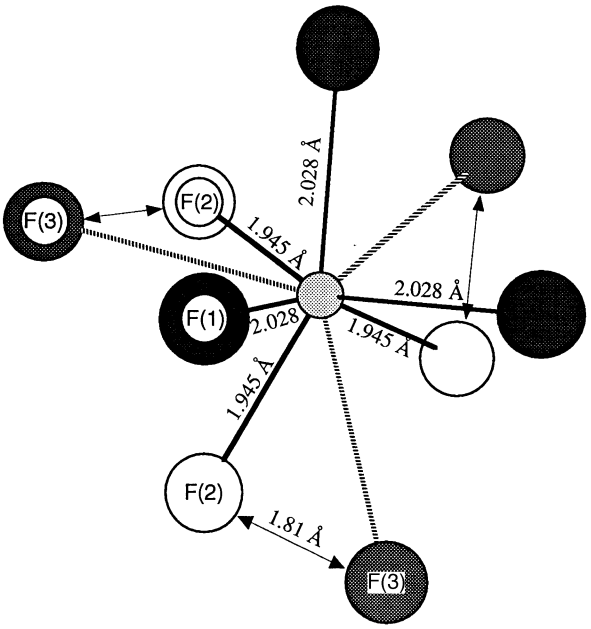

Fig. 3 Environment of the Zr^{4+} ion by the anionic species

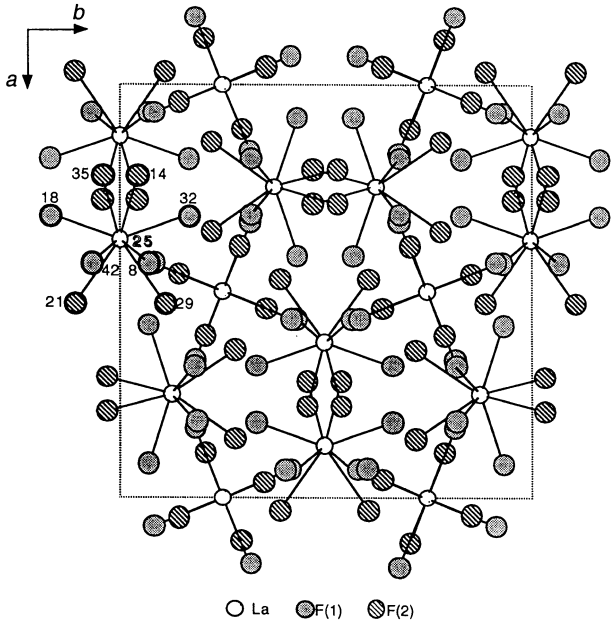

Fig. 4 Partial view of the structure of $La_3Zr_4F_{25}$ showing the La^{3+} polyhedra arrangement

and more recently β-$BaZr_2F_{10}$.[9] But in our case the use of anisotropic thermal coefficients did not remove the entire electron density around the Zr atoms. Therefore it seems more likely that the anionic environment around the Zr(2) atom is dynamically disordered, as is the case in $(NH_4)_3AlF_6$[10] or in $(NH_4)_3ZrF_7$[11,12] around Al^{3+} and Zr^{4+} respectively. So, although the reality seems to correspond to a dynamical model, we used multiple partially occupied sites leading to ineluctable short F–F distances to describe the Zr(2) environment. Of course, we introduced electron density corresponding to peaks appearing in the difference Fourier map, this was done with F(19), F(20), F(21) and F(22) (see Table 4). Probably no meaning should be attached to these refined positions, other than that it is a convenient way to describe the continuous average electron density resulting from the disorder. This disorder is not only a rotational disorder but also affects the centre of mass [Zr(2) atom] of the polyhedron since this

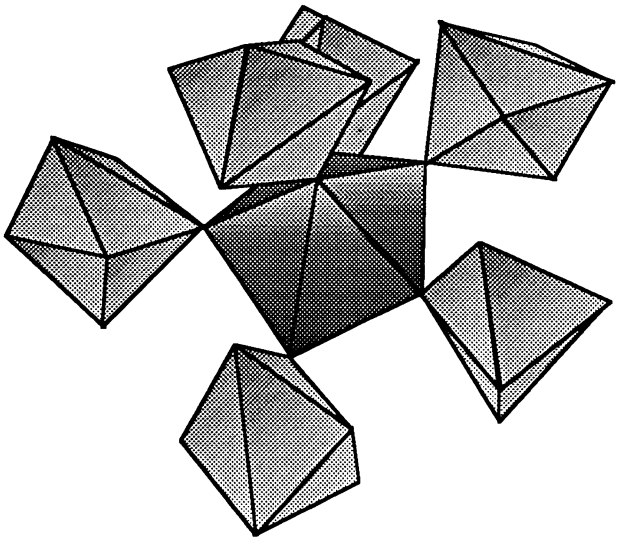

Fig. 5 Linking of Zr octahedra and La dodecahedra in $La_3Zr_4F_{25}$

position is much better described by a splitting of the corresponding site. Otherwise the temperature factor of the Zr(2) atom would reach a very high value. Therefore the description of the Zr(2) polyhedron in Table 5 is nothing more than an average possible configuration at a given instant and must be considered as such. For simplification, in the description, we have excluded from this environment both F(20) and F(21) because they participate only in the coordination of Zr(2) and are mutually exclusive with F(19) and F(22). Both F(19) and F(22) are corners shared between Zr(2) and Zr(1), and Zr(2) and Zr(3) respectively.

Europium spectroscopy

The Eu^{3+} fluorescence and excitation spectra have been recorded at 77 K; the $^5D_0$, $^5D_1$ and $^7F_{1,4}$ levels were investigated. Three spectra could be isolated using three different sets of excitation/emission lines and were assigned to three different sites. The more characteristic spectra are displayed in Fig. 6–9. The $^5D_0 \rightarrow {}^7F_{1,2}$ emission spectra are displayed in Fig. 6. Spectrum sp 2 could be easily isolated by excitation within the $^5D_0$ level at 17325 cm^{-1}. The emission lines for sp 3 were extracted under more drastically selective excitation at 17303 cm^{-1}, the excitation line width having been narrowed by a Fabry–Perrot filter. On the other hand, excitation without this filter at 17300 cm^{-1} resulted in mixed emission (sp 1 and sp 3), whereas sp 1 was isolated after selective excitation within the $^5D_1$ level at 19064 cm^{-1}. The $^7F_0 \rightarrow {}^5D_1$ excitation spectra monitored at 16298 cm^{-1} (sp 1 and 2), 16330 cm^{-1} (sp 2) and 16430 cm^{-1} (sp 3) are displayed in Fig. 7. One main excitation component may be assigned to sp 1 (19064 cm^{-1}) and sp 3 (19042 cm^{-1}), whereas there is a coincidence of excitation lines for sites 1 and 2 at 19073 cm^{-1}. For the first monitoring wavenumber, a time-resolution effect is observed; the relative intensity of the line at 19073 cm^{-1} increases with respect to that at 19604 cm^{-1} when the measurement is carried out at longer delays after the excitation pulse. This effect traduces energy transfer from the corresponding site 2 towards site 1. The $^7F_0 \rightarrow {}^5D_0$ excitation spectra monitored at 16888 cm^{-1} (sp 1), 16330 cm^{-1} (sp 2) and 16430 cm^{-1} (sp 3) are displayed in Fig. 8. The $^7F_0 \rightarrow {}^5D_0$ lines for sp 1 and 3 appear at almost the same wavenumber (17300, 17303 cm^{-1}) whereas for sp 2 it is shifted to 17325 cm^{-1}. Both lines (17300, 17325 cm^{-1}) appear in the first two spectra, due to coincidence of the emissions at the monitoring wavelengths. Taking the relative intensities into consideration allows the assignment of each of them to sp 1 and 2 respectively. The selectively excited emission spectra in the $^5D_0 \rightarrow {}^7F_4$ transition range are displayed in Fig. 9. The $^5D_0$

Table 4 Positional parameters and isotropic thermal parameters for α-$LaZr_3F_{15}$

atom	Wyckoff position	occupancy	x	y	z	B_{iso} or B_{eq}/Å
La(1)	4f	1	0.28223(4)	0	0.20982(7)	0.54(1)
La(2)	4e	1	0	0.26912(3)	0.22195(7)	0.50(1)
Zr(1)	2a	1	1/2	1/2	0.8708(2)	0.63(2)
Zr(2)	4f	0.50	0.5139(1)	1/2	0.3752(2)	0.86(4)
Zr(3)	8g	1	0.32430(5)	0.33776(4)	0.43549(8)	0.96(1)
Zr(4)	4f	1	0.36524(6)	0	0.7103(1)	0.49(1)
Zr(5)	4c	1	1/4	1/4	0	0.49(1)
Zr(6)	4e	1	0	0.33199(5)	0.7184(1)	0.58(1)
F(1)	4f	1	0.1276(5)	0	0.127(1)	2.2(1)
F(2)	8g	1	0.4087(3)	0.0888(3)	0.2367(6)	2.10(9)
F(3)	8g	1	0.0944(3)	0.3874(3)	0.2254(7)	1.71(8)
F(4)	4e	1	0	0.1217(4)	0.1334(9)	1.8(1)
F(5)	8g	1	0.4155(4)	0.2608(3)	0.3163(7)	3.3(1)
F(6)	4e	1	0	0.3446(4)	0.4853(8)	1.8(1)
F(7)	8g	1	0.2656(4)	0.1356(3)	0.0766(7)	2.0(1)
F(8)	8g	1	0.2101(4)	0.0929(4)	0.3834(6)	3.8(1)
F(9)	4f	1	0.8618(5)	1/2	0.5243(7)	1.6(1)
F(10)	8g	1	0.1306(3)	0.2395(3)	0.0718(8)	2.4(1)
F(11)	8g	1	0.2429(4)	0.4231(3)	0.3327(7)	2.2(1)
F(12)	8g	1	0.2766(4)	0.2914(4)	0.2175(7)	3.0(1)
F(13)	2b	1	0	1/2	0.324(1)	1.5(2)
F(14)	2a	1	0	0	0.883(1)	2.1(2)
F(15)	4f	1	0.3257(5)	0	0.9377(8)	1.6(1)
F(16)	4e	1	0	0.3064(5)	0.9480(8)	2.2(1)
F(17)	8g	1	0.0950(4)	0.1982(4)	0.3974(7)	4.0(1)
F(18)	8g	0.75	0.7075(7)	0.7886(6)	0.490(1)	6.9(2)
F(19)	4f	0.50	0.4771(8)	1/2	0.630(2)	2.3(3)
F(20)	8g	0.30	0.116(1)	0.038(1)	0.484(3)	2.8(4)
F(21)	8g	0.30	0.445(1)	0.394(1)	0.513(3)	3.0(4)
F(22)	8g	0.85	0.4105(6)	0.4162(5)	0.338(1)	6.4(3)

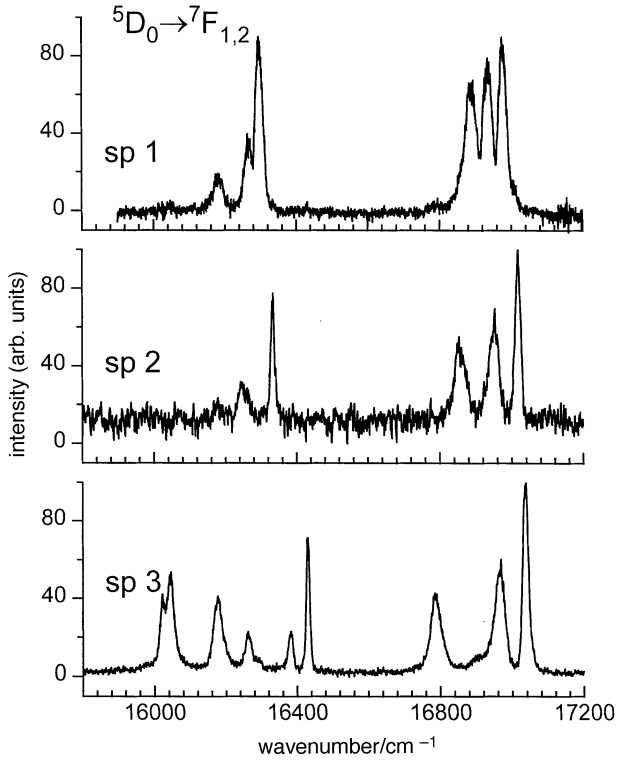

Fig. 6 $^5D_0 \rightarrow {}^7F_{1,2}$ emission spectra recorded at 77 K, on α-$LaZr_3F_{15}$:Eu^{3+}, under excitation at: 19064 cm^{-1} (sp 1) [the spectrum is the difference (data at long delay after pulse-data at short delay) calculated in order to remove the $^5D_1 \rightarrow {}^7F_{3,4}$ emissions]; 17325 cm^{-1} (sp 2); 17303 cm^{-1} (sp 3)

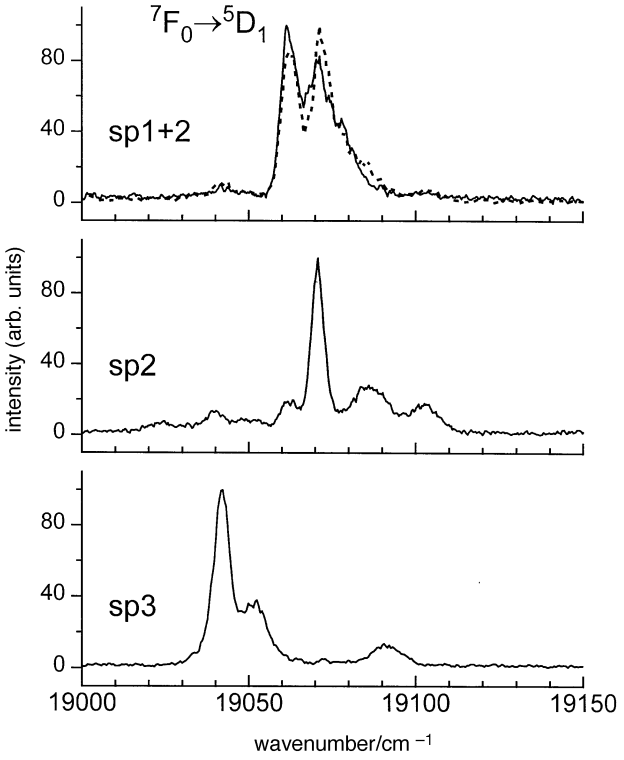

Fig. 7 $^7F_0 \rightarrow {}^5D_1$ excitation spectra recorded at 77 K, on α-$LaZr_3F_{15}$:Eu^{3+} monitored at: 16298 cm^{-1} (sp 1+2), with time resolution [full line: delay = 200 μs, gate = 900 μs; dashed line: delay = 2 μs, gate = 4 μs]; 16330 cm^{-1} (sp 2); 16430 cm^{-1} (sp 3)

lifetimes measured under direct excitation for sites 2 and 3 are equal to 7.3 and 6.6 ms respectively. The $^5D_0$ lifetime for site 1, measured on the long time decay of the transient curve after $^5D_1$ excitation, is equal to 8.4 ms; all these values are in good agreement with those reported for Eu^{3+} in fluorinated matrices.[1]

Discussion

From the investigation by optical spectroscopy, it is concluded unambiguously that europium ions are present on three different sites in the orthorhombic variety of $LaZr_3F_{15}$. As is usually observed, the europium is first expected to be substituted for

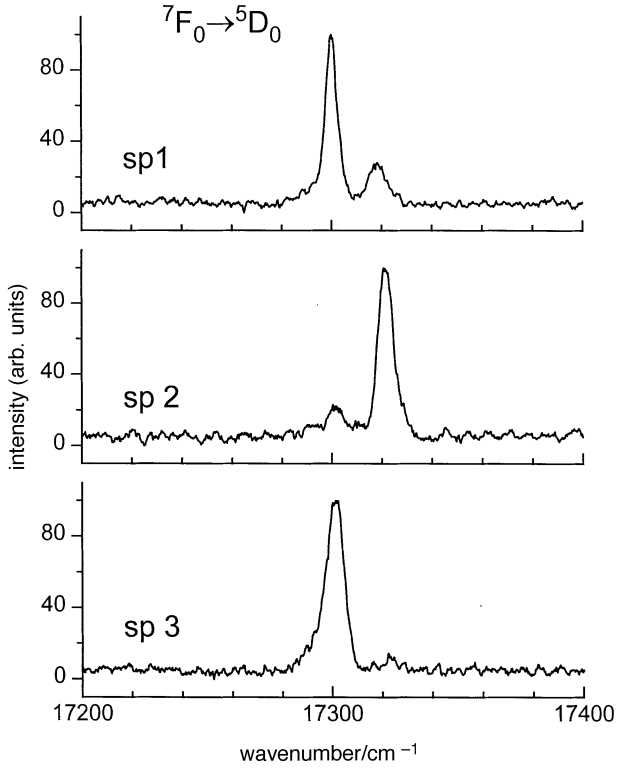

Fig. 8 $^7F_0 \rightarrow {}^5D_0$ excitation spectra recorded at 77 K, on α-$LaZr_3F_{15}$:Eu^{3+} monitored at: 16888 cm^{-1} (sp 1+2); 16330 cm^{-1} (sp 2+1); 16430 cm^{-1} (sp 3+2)

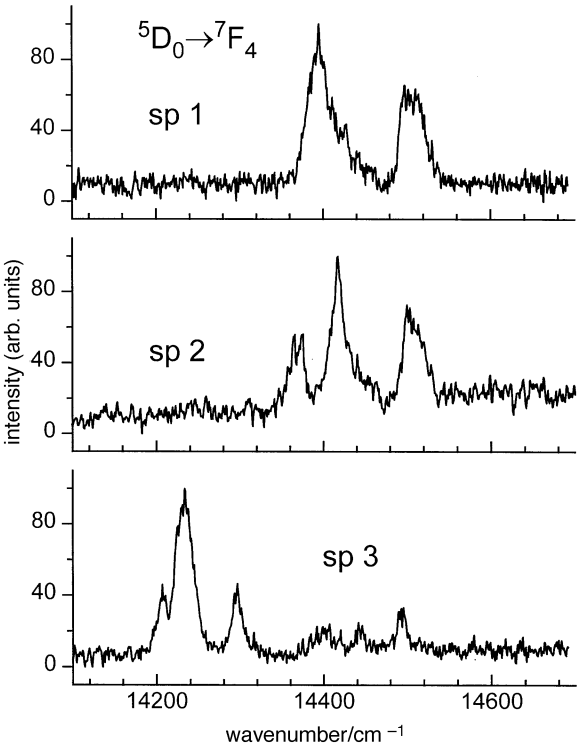

Fig. 9 $^5D_0 \rightarrow {}^7F_4$ emission spectra recorded at 77 K, on α-$LaZr_3F_{15}$:Eu^{3+} under excitation at: 19064 cm^{-1} (sp 1); 17325 cm^{-1} (sp 2); 17303 cm^{-1} (sp 3)

the two lanthanum sites of the structure, and under these conditions the third spectrum might be assigned to Eu^{3+} ions on one of the Zr^{4+} cationic sites. A statistical distribution between Bi^{3+} and Zr^{4+} on a cationic site has already been encountered in trigonal $BiZr_3F_{15}$.[13] The ionic radii of Bi^{3+}

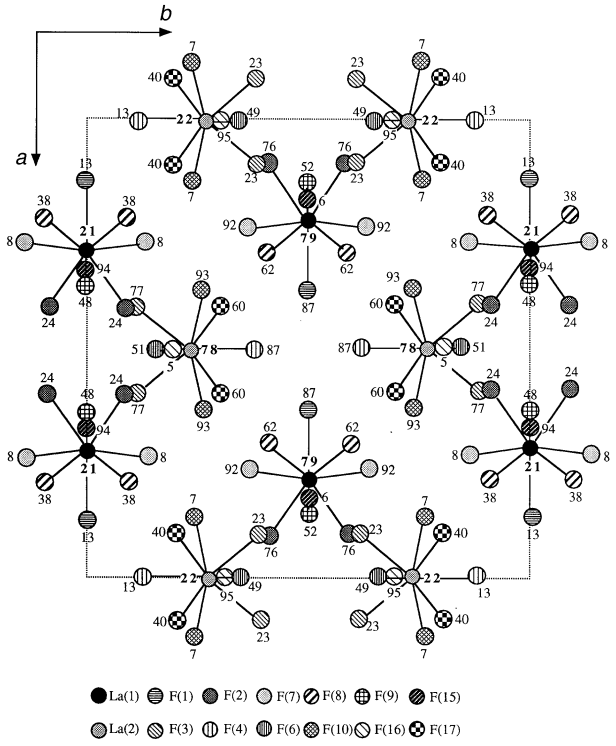

Fig. 10 Partial projection down [0 0 1] of the structure of α-$LaZr_3F_{15}$ showing the La^{3+} repartition and environments

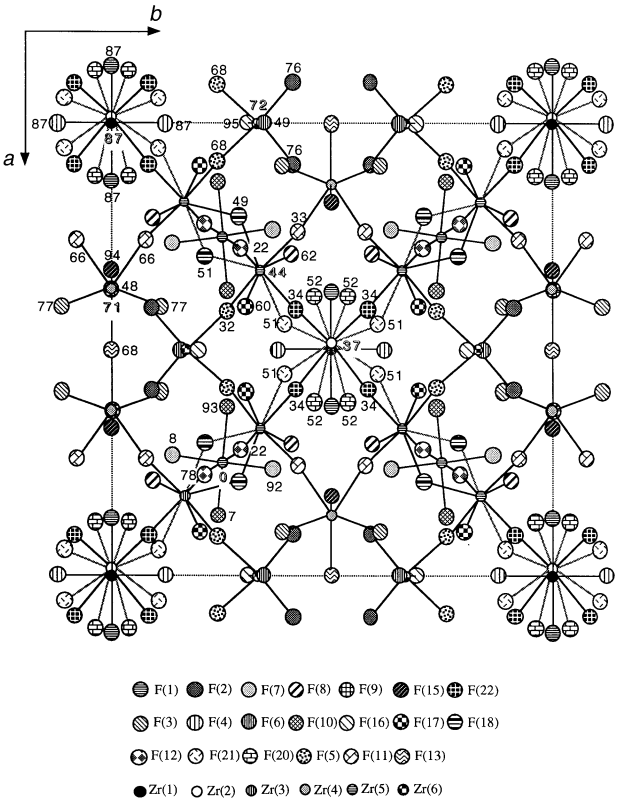

Fig. 11 Partial projection down [0 0 1] of the structure of α-$LaZr_3F_{15}$ showing the arrangement of the Zr^{4+} polyhedra

and Eu^{3+} (1.11 and 1.07 Å respectively)[7] are close enough to assume that this Eu^{3+}/Zr^{4+} substitution occurs easily.

Fig. 10 displays the coordination polyhedra around the two lanthanum sites. Both $La(1)^{3+}$ and $La(2)^{3+}$ independent cations are encompassed in tricapped trigonal prisms within which the mean La–F distances (see Table 5) are shorter than expected from Shannon's value.[7] These polyhedra are isolated

Table 5 Main interatomic distances (Å) and angles (°) in α-$LaZr_3F_{15}$

La(1) polyhedron [9] [mean La(1)–F = 2.467 Å]									
La(1)	F(8)	F(8)	F(15)	F(2)	F(2)	F(7)	F(7)	F(1)	F(9)
F(8)	**2.393(6)**	3.030(9)	4.443(9)	4.480(9)	3.360(9)	4.619(8)	2.819(8)	2.944(9)	2.931(9)
F(8)	78.6(2)	**2.393(6)**	4.443(9)	3.360(9)	4.480(9)	2.819(8)	4.619(8)	2.944(9)	2.931(9)
F(15)	136.2(2)	136.2(2)	**2.395(6)**	3.188(8)	3.188(8)	2.674(6)	2.674(6)	3.499(9)	4.574(9)
F(2)	134.2(2)	87.4(2)	81.9(2)	**2.471(5)**	2.896(7)	2.733(8)	4.502(7)	4.743(9)	2.590(7)
F(2)	87.4(2)	134.2(2)	81.9(2)	71.8(2)	**2.471(5)**	4.502(7)	2.733(8)	4.743(9)	2.590(7)
F(7)	141.9(2)	70.4(2)	66.3(1)	66.8(2)	130.2(2)	**2.493(5)**	4.420(6)	3.126(7)	4.302(8)
F(7)	70.4(2)	141.9(2)	66.3(1)	130.2(2)	66.8(2)	124.9(2)	**2.493(5)**	3.126(7)	4.302(8)
F(1)	73.4(2)	73.4(2)	90.5(3)	143.0(1)	143.0(1)	77.0(1)	77.0(1)	**2.530(7)**	4.714(9)
F(9)	72.3(2)	72.3(2)	134.3(2)	61.8(2)	61.8(2)	116.4(1)	116.4(1)	135.2(3)	**2.568(6)**

La(2) polyhedron [9] [mean La(2)–F = 2.448 Å]									
La(2)	F(16)	F(17)	F(17)	F(3)	F(3)	F(10)	F(10)	F(4)	F(6)
F(16)	**2.391(7)**	4.441(9)	4.441(9)	3.069(8)	3.069(8)	2.548(7)	2.548(7)	3.394(10)	4.576(9)
F(17)	136.0(2)	**2.400(6)**	2.987(9)	3.408(8)	4.525(8)	2.884(9)	4.536(9)	2.958(9)	2.910(9)
F(17)	136.0(2)	77.0(2)	**2.400(6)**	4.525(8)	3.408(8)	4.536(9)	2.884(9)	2.958(9)	2.910(9)
F(3)	79.0(2)	89.7(2)	138.9(2)	**2.433(5)**	2.968(7)	2.794(7)	4.471(7)	4.643(8)	2.738(8)
F(3)	79.0(2)	138.9(2)	89.7(2)	75.2(2)	**2.433(5)**	4.471(7)	2.794(7)	4.643(8)	2.738(8)
F(10)	63.4(2)	72.8(2)	138.0(2)	69.7(2)	132.1(2)	**2.460(6)**	4.105(7)	2.859(7)	4.395(9)
F(10)	63.4(2)	138.0(2)	72.8(2)	132.1(2)	69.7(2)	113.1(2)	**2.460(6)**	2.859(7)	4.395(9)
F(4)	87.5(3)	73.9(2)	73.9(2)	139.5(1)	139.5(1)	70.1(1)	70.1(1)	**2.516(7)**	4.691(9)
F(6)	136.3(3)	72.1(2)	72.1(2)	66.8(2)	66.8(2)	123.0(1)	123.0(1)	136.2(2)	2.541(7)

Zr(1) polyhedron [6] [mean Zr(1)–F = 2.020 Å]						
Zr(1)	F(4)	F(4)	F(1)	F(1)	F(19)	F(14)
F(4)	**1.984(6)**	3.968(9)	2.822(7)	2.822(7)	2.84(1)	2.897(9)
F(4)	177.9(3)	**1.984(6)**	2.822(7)	2.822(7)	2.84(1)	2.897(9)
F(1)	90.0(0)	90.0(0)	**2.006(7)**	4.012(9)	2.63(1)	2.871(10)
F(1)	90.0(0)	90.0(0)	178.8(4)	**2.006(7)**	3.14(1)	2.871(10)
F(19)	89.0(2)	89.0(2)	80.6(4)	100.7(4)	**2.065(10)**	4.1(1)
F(14)	91.0(2)	91.0(2)	89.4(3)	89.4(3)	170.0(4)	**2.076(9)**

Zr(2) polyhedron [6] [mean Zr(2)–F = 2.052 Å]						
Zr(2)	F(22)	F(22)	F(22)	F(22)	F(19)	F(14)
F(22)	**1.838(8)**	2.73(1)	3.92(1)	2.81(1)	3.32(2)	2.71(1)
F(22)	159.8(5)	**1.838(8)**	3.92(1)	2.81(1)	3.32(2)	2.71(1)
F(22)	89.6(3)	96.0(4)	**2.146(9)**	2.73(1)	3.00(2)	2.71(1)
F(22)	79.1(3)	89.6(4)	159.8(5)	**2.146(9)**	3.00(2)	2.71(1)
F(19)	101.3(4)	97.3(5)	97.3(5)	101.3(4)	**2.153(13)**	4.34(1)
F(14)	77.3(4)	84.0(4)	84.0(4)	77.3(4)	178.1(4)	**2.192(2)**

Zr(3) polyhedron [7] [mean Zr(3)–F = 2.065 Å]							
Zr(3)	F(8)	F(17)	F(22)	F(11)	F(18)	F(12)	F(5)
F(8)	**1.976(6)**	2.496(10)	3.022(13)	2.521(8)	2.495(9)	2.866(8)	4.000(9)
F(17)	152.5(1)	**1.985(6)**	2.909(13)	3.949(9)	3.211(10)	3.829(9)	2.511(9)
F(22)	97.7(4)	78.1(2)	**2.036(9)**	2.638(10)	4.027(10)	3.099(11)	2.541(9)
F(11)	76.8(2)	92.7(3)	79.7(3)	**2.080(6)**	2.712(8)	2.416(8)	3.793(9)
F(18)	75.4(3)	103.5(3)	160.5(3)	80.9(2)	**2.100(9)**	2.415(7)	2.556(11)
F(12)	140.9(3)	137.3(3)	96.3(4)	70.1(2)	79.3(3)	**2.126(6)**	2.390(9)
F(5)	151.2(2)	74.6(2)	74.6(3)	127.2(3)	120.0(2)	67.9(2)	**2.154(6)**

Zr(4) polyhedron [7] [mean Zr(4)–F = 2.065 Å]							
Zr(4)	F(9)	F(3)	F(3)	F(15)	F(13)	F(11)	F(11)
F(9)	**1.980(6)**	3.197(7)	3.197(7)	3.940(9)	2.75(9)	2.625(8)	2.625(8)
F(3)	106.1(1)	**2.017(4)**	4.721(7)	2.616(7)	2.503(6)	2.570(7)	3.976(7)
F(3)	106.1(1)	131.1(2)	**2.017(4)**	2.616(7)	2.503(6)	3.976(7)	2.570(7)
F(15)	160.5(3)	80.8(2)	80.8(2)	**2.018(6)**	3.519(9)	2.817(8)	2.817(8)
F(13)	83.8(4)	74.0(2)	74.0(2)	115.7(4)	**2.138(2)**	4.019(6)	4.019(6)
F(11)	79.0(2)	76.3(2)	145.9(2)	85.2(2)	139.7(2)	**2.142(6)**	2.506(8)
F(11)	79.0(2)	145.9(2)	76.3(2)	85.2(2)	139.7(2)	71.6(2)	**2.142(6)**

Zr(5) polyhedron [6] [mean Zr(5)–F = 1.989 Å]						
Zr(5)	F(10)	F(10)	F(7)	F(7)	F(12)	F(12)
F(10)	**1.980(5)**	3.960(7)	2.717(7)	2.893(8)	2.738(8)	2.888(8)
F(10)	180.0(0)	**1.980(5)**	2.893(8)	2.717(7)	2.888(8)	2.738(8)
F(7)	86.4(2)	93.6(2)	**1.989(5)**	3.977(7)	2.809(7)	2.831(8)
F(7)	93.6(2)	86.4(2)	180.0(0)	**1.989(5)**	2.831(8)	2.809(7)
F(12)	87.0(2)	93.0(2)	89.5(2)	90.5(2)	**1.999(5)**	3.999(8)
F(12)	93.0(2)	87.0(2)	90.5(2)	89.5(2)	180.0(0)	**1.999(5)**

Table 5 (*continued*)

Zr(6) polyhedron [6] [mean Zr(6)–F = 1.993 Å]

Zr(6)	F(2)	F(2)	F(6)	F(16)	F(5)	F(5)
F(2)	**1.966(5)**	2.869(7)	2.956(8)	2.716(8)	2.884(8)	3.993(8)
F(2)	93.7(2)	**1.966(5)**	2.956(8)	2.716(8)	3.993(8)	2.884(8)
F(6)	97.1(2)	97.2(2)	**1.978(6)**	3.954(9)	2.742(9)	2.742(9)
F(16)	86.9(2)	86.9(2)	173.8(3)	**1.982(7)**	2.818(9)	2.818(9)
F(5)	92.2(2)	172.8(2)	86.2(2)	89.1(2)	**2.034(6)**	2.657(9)
F(5)	172.8(2)	92.2(2)	86.2(2)	89.1(2)	81.5(3)	**2.034(6)**

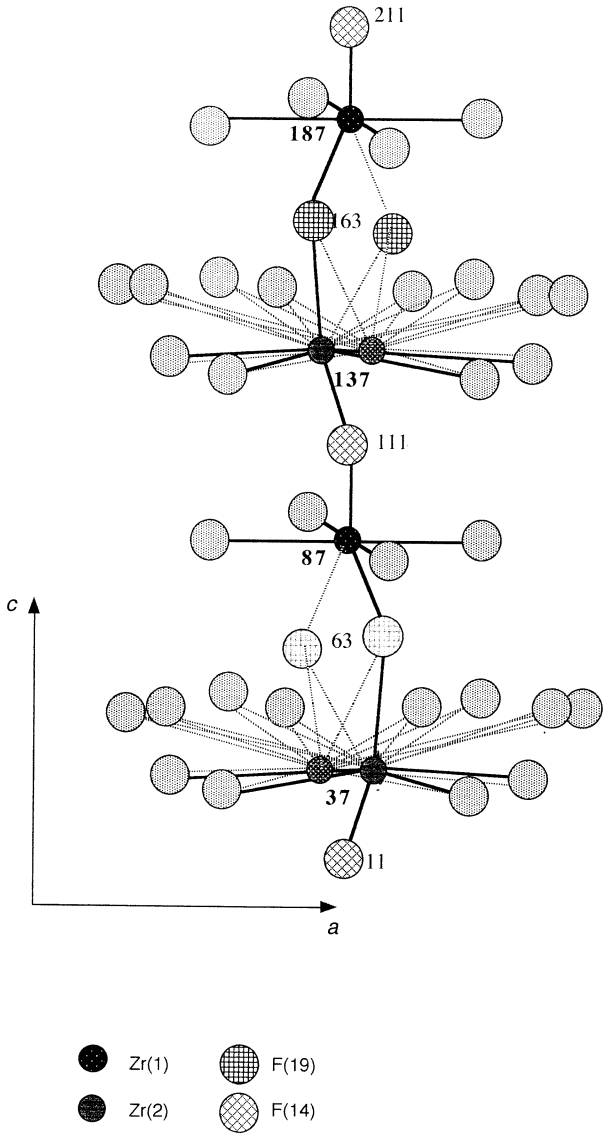

Fig. 12 Partial view showing the detail of the string of both Zr(1) and Zr(2) polyhedra along the [0 0 1] direction

relative to each other and the shortest La(2)–La(2) distance between neighbouring rare earth ions is greater than 6 Å. The point symmetries at the two sites are C_s. The point symmetries at the Zr^{4+} sites are also C_s, except that of Zr(1) which is C_{2v}. Each of the three spectra exhibits three $^5D_0 \rightarrow {}^7F_1$ components of approximately the same intensity, which rules out C_{2v} symmetry, but it is still impossible to choose between the other possible locations. Sp 1 and 2 are qualitatively rather similar so that they could be assigned to the two lanthanide sites which may be described with almost the same geometrical arrangement and distances of the first neighbours. Spectrum 3 would then be assigned to Eu^{3+} on one of the Zr^{4+} sites, more probably one of the seven-coordinate ones.

There are six crystallographically independent Zr^{4+} ions (see Table 4). Both Zr(3) and Zr(4) are seven-coordinated by the fluorine ions. Zr(1), Zr(5) and Zr(6) are in slightly distorted octahedral coordination (Fig. 11). As mentioned previously, the anionic environment around Zr(2) atom is dynamically disordered. In spite of these multiple anionic positions that are mutually exclusive, we consider the primarily coordination of the Zr(2) as being distorted octahedral. A careful examination of the possible motion of the $[Zr(2)F_6]^{2-}$ anion shows that this polyhedron would precess about the F(14)–F(19) direction, the F(14) corner behaving as a fixed point since the temperature factor for the F(14) is not really high and the corresponding site is not split, in contrast to both Zr(2) and F(19) (see Fig. 12). The structure described is characterised by a number of different $[ZrF_6]^{2-}$ and $[ZrF_7]^{3-}$ corner-sharing polyhedra. This is also qualitatively in agreement with the Raman scattering spectrum described in ref. 1, where the complex structure and the large width of the high frequency bands, directly related to the Zr^{4+} environments, was proposed.

Conclusion

The crystal structures of both $La_3Zr_4F_{25}$ and α-$LaZr_3F_{15}$ fluorides have been determined from single-crystal X-ray diffraction data. The structures were also investigated using Eu^{3+} as a local structural probe and correlations between Eu^{3+} luminescence and structures were discussed. $La_3Zr_4F_{25}$ is characterised by some anions out of regular positions, whereas α-$LaZr_3F_{15}$ corresponds more likely to a dynamical anionic disorder. More precise anionic location will be investigated using neutron diffraction.

References

1 S. J. L. Ribeiro, P. Dugat, D. Avignant and J. Dexpert-Ghys, *J. Non-Cryst. Solids*, 1996, **8**, 197.
2 B. A. Frenz, *Computing in crystallography*, ed. H. Shenk, R. Olthof-Hazekamp, H. Van Koningveld and G. C. Bassi, Delft University Press, Delft, The Netherlands, 1982.
3 A. Zalkin, D. Eimerl and S. P. Velsko, *Acta Crystallogr., Sect. C*, 1988, **44**, 2050.
4 R. Papiernik and B. Frit, *Mater Res. Bull.*, 1984, **19**, 509.
5 A. Mikou, J. P. Laval and B. Frit, *Rev. Chim. Miner*, 1987, **24**, 315.
6 G. Brunton, *Acta Crystallogr., Sect. B*, 1971, **27**, 245.
7 R. D. Shannon, *Acta Crystallogr., Sect. A*, 1976, **32**, 751.
8 J. P. Laval and B. Frit, *Acta Crystallogr., Sect. B*, 1980, **36**, 2533.
9 J. P. Laval, B. Frit and J. Lucas, *J. Solid State Chem.*, 1988, **72**, 181.
10 E. G. Steward and H. P. Rookby, *Acta Crystallogr.*, 1953, **6**, 49.
11 H. J. Hurst and J. C. Taylor, *Acta Crystallogr., Sect. B*, 1970, **26**, 417.
12 H. J. Hurst and J. C. Taylor, *Acta Crystallogr., Sect. B*, 1970, **26**, 2136.
13 E. Caignol, J. Metin, R. Chevalier, J. C. Cousseins and D. Avignant, *Eur. J. Solid State Inorg. Chem.*, 1988, **25**, 399.

Paper 7/08080H; *Received* 10*th November*, 1997